Original Article

Biogenic Ag–Cu Nanoparticles Synthesized with Extract of *Eryngium Billardieri* L. and Evaluation of their Anticancer Potential on PC-3 and LNCaP Cancer Cell Lines

Zahra Ebrahim†, Ghazaleh Feyzabadi†, Nastaran Asghari Moghaddam, Azadeh Mohammadgholi

Department of Biology, CT. C., Islamic Azad University, Tehran, Iran

†These authors contributed equally to this work.

Abstract

Background: The anticancer action of biogenic Ag-Cu nanoparticles (NPs) using *Eryngium billardieri* against PC-3 and LNCaP cell lines in prostate malignancy was investigated.

Materials and Methods: XRD, FTIR, EDAX, FESEM, and TEM were used to illustrate the Ag–Cu NPs. The PC-3 and LNCaP cell lines were used to test the anticancer ability of Ag–Cu NPs. The cytotoxicity was assessed by MMT and flow cytometry. Apoptotic and metastatic-promoting gene expressions were evaluated by real-time PCR. ROS generation was measured.

Results: NPs are spherical and their average size was 12 ± 9.7 nanometers. The EDAX result indicated the presence of Ag, Cu, and C. The XRD results revealed the NPs' crystalline structure. The results demonstrated a remarkable antiproliferative effect of the nanoparticles, with IC50 values of 15.43 µg/mL for PC-3 and 7.64 µg/mL for LNCaP. The Ag–Cu NPs exhibited a tendency to trigger apoptosis. This was confirmed by analyzing apoptosis-related gene expression. The apoptotic influence of Ag–Cu NPs was suggested to be critical when compared to the control and extract-treated groups by the up-regulation of *Bcl2*-related X (*Bax*), *caspase3*, and *caspase9*, and the down-regulation of *Bcl2*. Furthermore, Annexin V-FITC/propidium iodide presented a 23.15% and 22.3% apoptotic ratio of PC-3 and LNCaP cells, respectively. Vascular endothelial growth factor (*VEGF*), and metalloproteinases (MMPs) down-regulation showed that Ag–Cu NPs were hostile to metastasis. Also, ROS generation was estimated at 1261 and 1366 RFU in LNCaP and PC-3 cells treated with green-synthesized Ag–Cu NPs, respectively.

Conclusions: The study suggested *E. billardieri* synthesized Ag–Cu as a potential candidate in prostate cancer therapeutic management.

Keywords: Angiogenesis, apoptosis, caspases, *Eryngium*, metal nanoparticles, neoplasm metastasis, prostate neoplasms

Address for correspondence: Dr. Nastaran Asghari Moghaddam, Department of Biology, CT. C., Islamic Azad University, Tehran, Iran.
E-mail: nas.asgharimoghaddam@iauctb.ac.ir
Submitted: 02-Jun-2024; **Revised:** 08-Jul-2024; **Accepted:** 09-Jul-2024; **Published:** 31-May-2025

Introduction

Prostate cancer (PC) remains a significant health concern for men worldwide. It typically develops in the prostate gland, a small, walnut-sized organ in the male reproductive system. Prostate cancer often progresses slowly and may not show symptoms in its early stages. Regular screening, including digital rectal exams and prostate-specific antigen (PSA) tests, was crucial for early detection. Treatment options included surgery, radiation therapy, hormone therapy, and chemotherapy, contingent on the cancer's stage and severity, which often leads to unwanted side effects. Hence, research and advancements in prostate cancer diagnosis and treatment are ongoing, with an increasing focus on personalized medicine, immunotherapy, and targeted therapies.[1,2] The ability of nanoparticles (NPs) to specifically target solid tumors by utilizing the enhanced

Access this article online

Quick Response Code:

Website: www.advbiores.net

DOI: 10.4103/abr.abr_255_24

How to cite this article: Ebrahim Z, Feyzabadi G, Asghari Moghaddam N, Mohammadgholi A. Biogenic Ag–Cu nanoparticles synthesized with extract of *Eryngium billardieri* L. and evaluation of their anticancer potential on PC-3 and LNCaP cancer cell lines. Adv Biomed Res 2025;14:43.

permeability and retention phenomenon within tumors presents a potential treatment option for PC.[3] Their small size enables NPs to evade the unintended side effects often associated with non-targeted therapies when administered systemically, all while enhancing the effectiveness of the encapsulated anticancer agents. Additionally, NPs can actively target particular tissues when paired with molecules that target receptors; this is advantageous when it comes to reaching PC tissue as it targets multiple upregulated biomarkers found in PC cells. One prominent instance is the overexpression of the prostate-specific membrane antigen (PSMA), which can be up to a thousand times higher in malignant prostate epithelium compared to normal tissues.[4,5] Through active targeting and controlled release, these nanoparticles aim to maximize the therapeutic impact on PC cells while minimizing harm to healthy tissues. This innovative use of nanotechnology showcases the potential for more effective and precise treatments, although further research and clinical testing are needed to fully realize their efficacy and safety in prostate cancer therapy.[3,6] Among all different metallic NPs, silver (Ag) and copper (Cu) NPs have garnered tremendous attention in the field of medicine.[7,8] Currently, Ag-NPs have been researched for their applications in antimicrobial agents, vaccine adjuvants, wound healing, bone regeneration, and dental equipment.[9] Several studies emphasized Ag NPs' effects against prostate cancer both *in vitro* and *in vivo*.[10–12] Copper (Cu) NPs have received ample interest in cancer therapy through angiogenesis and cell growth inhibition, as well as producing reactive oxygen species (ROS).[13–15] In total, the remarkable anticancer activity of Ag and Cu is associated with their ability to disrupt cancerous cell membranes and interfere with vital cellular processes and signaling pathways ending in apoptosis. The exact mechanisms by which silver and copper ions promote cell death are: (1) the generation of reactive oxygen species (ROS), (2) the interaction with DNA, (3) the disruption of mitochondrial function, and (4) the interaction with cell membrane components.[16,17] The synthesis of alloyed nanomaterials for example bimetallic Ag–Cu NPs, is beginning to gather great significance in the realm of cancer therapy. Several studies conducted by fabricated Ag–Cu NPs have exhibited their improved stability, elevated catalytic activity, and enhanced apoptotic properties.[18–23] It seems that the utilization of Ag–Cu NPs in prostate cancer therapy can represent a promising approach. The green synthesis method for NPs utilizes natural, non-toxic, and renewable materials, including plant extracts, microorganisms, and other biocompatible substances, serving as reducing agents or stabilizers during the nanoparticle synthesis process. This approach has garnered attention for its eco-friendly characteristics, cost-effectiveness, and capacity to yield NPs with diverse applications in fields such as medicine, electronics, and environmental science.[24] Considering herbs' ability to synthesize NPs, in the current study, *Eryngium billardieri* was used as the reductive agent to produce Ag–Cu NPs. *E. billardieri* belongs to the *Apiaceae* family and is known for its antidiabetic and antiinflammatory properties. Recent studies have also highlighted its apoptotic effects on various cancerous cells.[25–28]

This research sought the anticancer properties of Ag–Cu NPs synthesized by *E. billardieri* herbal extract. Using a green-synthesis approach, we aligned with the sustainable and ecofriendly trends in nanotechnology. Notably, we aimed to evaluate the cytotoxicity of our biogenic Ag–Cu NPs against PC-3 and LNCaP prostate cancer cell lines. Our study stands out due to some novel aspects. Originally, we employed biosynthesis by plant-derived compounds to produce ecofriendly NPs and minimize adverse environmental impacts. Second, doping silver and copper NPs enhanced their potential therapeutic efficiency. Finally, since PC-3 and LNCaP show different growth and metastatic activity, comparing their responses to the same nanoparticle, can provide more evidence of the capability of the synthesized Ag–Cu in different stages of PC for further studies.

Materials and Methods

Materials

Fetal bovine serum (FBS), 3-(4,5-Dimethylthiazol-2-yl) -2,5-diphenyltetrazolium bromide (MTT), Medium RPMI-1640, penicillin/streptomycin 100 X, phosphate-buffered saline (PBS), Trypsin- EDTA, and trypan blue, were acquired from Gibco (ThermoFisher Scientific, USA). Ag (NO_3) and Cu (NO_3) $_2$.6H_2O were bought from Merck (Germany). The dried leaves of *E. billardieri* were obtained from the Iranian Biological Resource Center. The HEK-293, LNCaP, and PC-3 cell lines were purchased from the Cell Bank of Pasteur Institute (Iran) and the National Cell Bank of Iran's Genetic and Biological Resource Center. The Annexin V/propidium iodide (PI) assay kit was from Roche (Germany). The RNA Qiagen extraction kit (USA), and the RevertAid First Strand cDNA Synthesis Kit (Lithuania) were used.

Eryngium billardieri leaf extract preparation

The *E. billardieri* plant, also known as "bouqenaq," was acquired from the Iranian Biological Resource Center (IBRC) under the herbarium code IBRC P1011605. To obtain the plant extract, the aerial parts of *E. billardieri* were first air-dried and subsequently completely desiccated in the shade for 10 days. The leaves were then powdered thoroughly using an electric mill and stored in glass containers. The extraction of the plant was performed through a Soxhlet method, utilizing the powdered plant material. A total of 50 g of leaf powder were placed in a thimble and added to the apparatus with 500 ml of distilled water over 12 h. After the extraction was done, the mixture was allowed to cool at ambient temperature. To remove debris, the extract was first filtered using Whatman No. 1 filter paper (Whatman plc, Kent, UK). Following, the filtrate was centrifuged at 4000 rpm for 15 min. Then, the supernatant was carefully collected and concentrated by a rotary evaporator (Rv10 digital, Germany) under reduced pressure at 40°C to remove the solvent. To further purify, the extract was subjected to double distillation by distilled water.

The resulting solid powder was concentrated to its final volume through double distillation using distilled water and stored at 4°C for subsequent investigation into its effects on cancer cells.

Ag–Cu synthesis

The green synthesis of Ag–Cu NPswas performed via a precipitation method using the reduction of copper and silver ions by the aqueous extract of *E. billardieri*. To prepare Ag–Cu NPs, 0.01 M of copper nitrate ($Cu(NO_3)_2.6H_2O$) and 0.1 M of silver nitrate ($AgNO_3$) were mixed in 100 mL of distilled water. Subsequently, 4–5 mL of the plant extract were added to the solution, and the mixture was continuously stirred for 24 h on a magnetic stirrer. The color change indicated the synthesis of Ag–Cu NPs. The resulting precipitate was washed three times with distilled water. All washing steps involved centrifugation at 13,000 rpm for 20 min. In the final washing step, ethanol was used, and the product was kept at 60°C for 2 h. Subsequently, the product was placed at 37°C for 4 h. The obtained dry powder was used for SEM, XRD, TEM, FT-IR, and EDAX analysis.

Characterization of Ag–Cu nanoparticles

The synthesized Ag–Cu NPs were characterized through various methods. The morphology and size of the NPs were assessed via scanning electron microscopy (SEM) using an FEI NOVA NANOSEM 450 at 15 kV and transmission electron microscopy (TEM) with a Zeiss EM900 instrument from Germany. The presence of functional groups and molecular binding properties in the extract and Ag–Cu NPs were confirmed using Fourier-transform infrared spectroscopy (FT-IR) within the wave number range of 400–4000 cm^{-1}. Elemental composition was analyzed using energy-dispersive X-ray spectroscopy (EDX) with a JSM-7500 Field Emission Scanning Electron Microscope from Japan. The crystallographic structure of Ag–Cu NPs was determined by an X-ray diffractometer (XRD) (Bruker AXS model D8 Advance using Cu Ka radiation within the range of 2θ =10°–90°).

Cell line preparation

In this study, PC-3 PC cells were obtained from the National Cell Bank of Iran's Genetic and Biological Resource Center. RPMI medium was used for the cultivation of these cells. LNCaP prostate cancer cells (C439) and HEK-293 (C634) kidney immortalized cell lines were acquired from the Pasteur Institute of Iran's cell bank. DMEM medium was used for the cultivation of these cell lines.

MTT cytotoxicity

To assess the cytotoxicity of the extract, a 3-(4,5-Dimethylthiazol-2-yl)-2,5-diphenyltetrazolium bromide (MTT) assay was conducted. Initially, PC-3, LNCap, and HEK-293 cells (as a non-tumorigenic origin control for selectivity analysis) were cultured in RPMI 1640 medium supplemented with 10% FBS. Incubation was carried out at 37°C for 24 h. Then, both cell lines were treated with the extract and incubated for 24, 48, and 72 h, separately. The same process was done for the treatment of cells with synthesized NPs. Different concentrations of both herbal extract and biogenic NPs, ranging from 3.5, 6, 12, 25, 50, 100 µg/mL, were used. For the MTT assay, cells were treated with 100 µL of MTT solution (5 mg/mL) and incubated at 37°C for 4 h. Afterward, the culture medium was removed, and 100 µL of dimethyl sulfoxide (DMSO) was added to each well. The mixture was then incubated for an additional 5 min at 25°C. The absorbance of the samples was measured at 570 nm using an ELISA Reader. Finally, the half-maximal inhibitory concentration (IC50) was calculated for all tested formulations.

Gene expression

Real-time PCR was used to investigate gene expression profiles of *VEGF, MMP2, MMP9, Bcl2, Bax, Caspase3,* and *Caspase9*. 1×10^6 PC-3 and LNCaP cells were cultured in each well, and treated with IC50 concentrations of the extract and NPs. After 24 h, RNA was extracted and converted into cDNA using the Revert AidTM First Strand cDNA Synthesis Kit (Fermentas). The RNA extraction process was performed by RiboEx Total RNA Kit (GENE ALL, South Korea) based on the manufacturer's instructions. Finally, the obtained cDNA was stored at − 20°C for further analysis. The amplification was performed in Rotor-Gene 6000 (Corbett Research, Australia) as follows: primary denaturation for 10 min at 95°C, 40 cycles for 20 s at 95°C, 20 s at 65°C, and 20 s at 72°C. Relative gene expression was calculated by $2^{-\Delta\Delta^{Ct}}$ compared with *ACTB* as the internal control. The designed primers were presented in Table 1.

Apoptosis assay

We used the Annexin V-FITC/PI double staining method to pursue the apoptotic effects of the extract and Ag–Cu NPs on the PC-3 and LNCaP cancer cell lines. The cells were given IC50 doses of extract and biogenic Ag–Cu for 24 h. Finally, the samples were examined using a machine called FACS Calibur made by Biosciences (USA).

Table 1: The primer sequences of the current study

Gene	Primer sequence (5′→3′)
ACTB	F: TCCTCCTGAGCGCAAGTAC
	R: CCTGCTTGCTGATCCACATCT
BAX	F: GAGCTGCAGAGGATGATTGC
	R: AAGTTGCCGTCAGAAAACATG
BCL2	F: ATTGGGAAGTTTCAAATCAGC
	R: CAGTCTACTTCCTCTGTGATGTTG
Caspase 3	F: CATACTCCACAGCACCTGGTTA
	R: ACTCAAATTCTGTTGCCACCTT
Caspase 9	F: CATATGATCGAGGACATCCAG
	R: TTAGTTCGCAGAAACGAAGC
MMP2	F: TTGACGGTAAGGACGGACTC
	R: CATACTTCACACGGACCACTTG
MMP9	F: GCACGACGTCTTCCAGTACC
	R: CAGGATGTCATAGGTCACGTAGC
VEGF	F: TGTCTAATGCCCTGGAGCCT
	R: GCTTGTCACATCTGCAAGTACG

Reactive oxygen species detection assay

The TPR-ROS Test Kit (TEB PAZHOUHAN RAZI) was used to measure ROS levels using a fluorescent dye DCFH-DA. In summary, PC-3 and LNCaP cell lines received a 24-h treatment with the IC50 doses of Ag–Cu NPs and the plant extract. The cells were washed in 100 µL buffer before treatment with 100 µL DCF for 60 min at 37°C. A total of 10 µL of R3 stimulator was added to the indicated positive control wells (H_2O_2), and the mixture was incubated for another 20 min at 37°C in the dark. After carefully removing the DCF staining buffer, 100 µL of the test buffer was added. The fluorescence intensity was measured at an excitation wavelength of 480–500 nm and an emission wavelength of 510–550 nm using a microplate reader.

Data analysis

To analyze the data, GraphPad Prism v. 8 was used. mean ± standard deviation (SD) was used to display the data. The statistical significance was estimated using a one-way analysis of variance and Tukey *post hoc* analysis. The predetermined level of statistical significance in every analysis was set at $\alpha = 0.05$.

Results

SEM and TEM Analysis

The morphological characteristics of *E. billardieri*-synthesized Ag–Cu bimetallic NPs were depicted by TEM and SEM. TEM microscopy results [Figure 1a] show that the doped NPs have nearly spherical structures and the average size is around 12 ± 9.7 nm. It should be noted that the size of NPs obtained from TEM is smaller than other size detector results, because of the dried form of NPs used for morphological analysis. The SEM image [Figure 1b] illustrates the three-dimensional structure of NPs with interconnected pores. The synthesized Ag–Cu composite nanostructures showed a non-uniform distribution of Ag–Cu. The aqueous extract's functional phytoconstituents interacted with these nanostructures, and the produced Ag–Cu's microstructure showed a smooth surface.

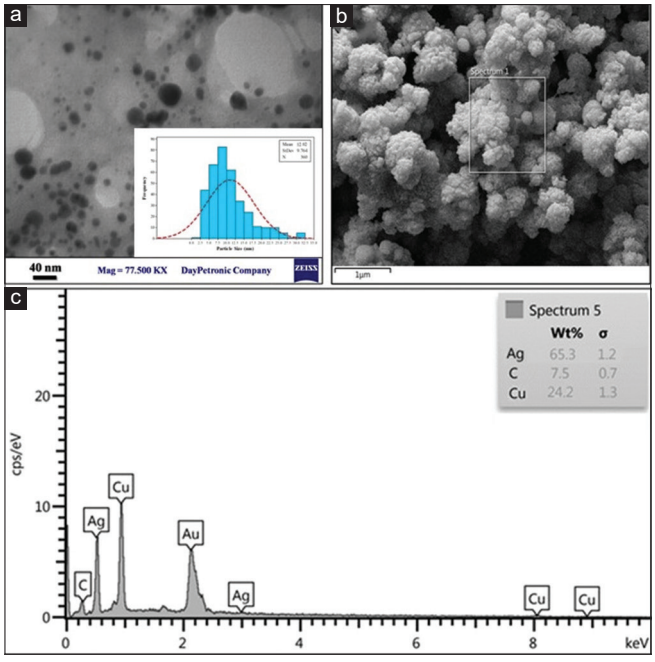

Figure 1: (a) TEM, (b) FE-SEM, and (c) EDAX of Ag–Cu NPs

EDX and EDS analysis

The elements used in the structure of the studied NPs are indicated by the peaks shown in this diagram. X-ray analysis was employed to identify these elements. In Figure 1c, this analytical method confirms the presence of silver and copper NPs. From the values of EDAX spectra, the stoichiometry confirmed the presence of elemental compositions: Copper (Cu), Carbon (C), and Silver (Ag). The observed result supports the incorporation of Ag into Cu, and it confirms the formation of Ag-doped Cu NPs. In the EDAX analysis for the elemental composition of the Ag–Cu NPs, the weight percentage of Cu, C, and Ag was reported as 24.2%, 7.5%, and 65.3%, respectively.

FTIR and XRD analysis

Infrared spectroscopy (FT-IR) is used to examine the absorption of radiation and analyze the vibrations in molecules and multi-atomic ions. The peak at 3436 cm^{-1} may indicate the stretching vibrations of alcohol and phenolic O-H groups. Another peak at 2078 cm^{-1} corresponds to C = N. The peak in the region at 1637 cm^{-1} is associated with C = C and C = O. The next peak at 641 cm^{-1} confirms the presence of alkanes and C-H bonds [Figure 2a]. According to the results obtained from FTIR spectroscopy, which is based on the absorption of radiation and the analysis of molecular vibrations, it is used for determining structures, measuring chemical species, and identifying organic compounds. The FTIR analysis concludes that the aqueous extract of the plant and the NPs have different interactions, resulting in distinct peaks. The presence of a peak in the region of 2942 cm^{-1} confirms the presence of alkene bonds. The peak at 2832 cm^{-1} indicates the presence of C = C and C-H carboxylic acid bonds. The peak in the region of 1740 cm^{-1} represents the C = O bond present in esters. The peak at 1423 cm^{-1} signifies aromatic bonds. Finally, the peak at 666 cm^{-1} confirms the presence of C-H bonds in alkenes and N-H bonds in amines [Figure 2b]. The XRD pattern was employed to assess the quality of the materials synthesized in this research. In this method, the crystal structure of the synthesized materials is examined through X-ray diffraction. Specifically, based on the 2θ values observed in the XRD pattern in the research results, it can be confirmed that NPs of silver copper exist at angles of 24, 28, 36, 47, 53, and 64 degrees [Figure 2c]. When Cu $(OH)_2$ and Ag are absent, the peaks show a good crystalline nature, which is explained by the X-ray diffraction pattern, which also confirmed the presence of Cu NPs.

Cytotoxicity

Utilizing the MTT assay, the viability of examined cells was assessed in response to varying concentrations of both synthesized NPs and extract. The MTT results in three

incubation times are depicted in Figure 3. Table 2 shows the IC50 values of Ag–Cu NPs and extract. Both NPs and extract induce cell death in a time- and dose-dependent manner. The high value of IC50 (approximately 190 µg/mL) for the treatments against HEK293 suggests a good biocompatibility of them [Figure 3a and b]. Furthermore, the cytotoxic effects of Ag-Cu NPs were significantly higher at each time of incubation than control and extract treated cells. The results, as shown in Figures 3b, and d, reveal a significant impact of Ag–Cu NPs on the PC-3 cell line compared to the control group. Notably, the effect of synthesized silver-copper NPs was more pronounced at a concentration of 100 µg/mL. Furthermore, at a concentration of 12.5 µg/mL, almost 50% of the cells survived after 24 h. In the case of the plant extract, at the concentration of 12.5 µg/mL, the survival rate of the cells was around 85%. The average IC50 value for the plant extract was 21.43 µg/mL, while for the synthesized NPs, it was 15.42 µg/mL. Similar tests were conducted on LNCaP PC cells, and the results, depicted in Figures 3e and f, demonstrated the Ag–Cu NPs' significant inhibitory effect on the growth and proliferation of cancer cells at all tested concentrations. The most substantial effect was observed at concentrations of 12.5, 25, 50, and 100 µg/mL. Only at concentrations of 50 and 100 µg/mL, the plant extract exhibited a slightly less pronounced but still acceptable effect compared to the control group ($P < 0.05$). The average IC50 values for Ag–Cu NPs and extract on LNCaP cells were found to be 7.64 µg/mL and 13.58 µg/mL, respectively. As the results present the biogenic NPs were more influential on cancerous cells than the extract. It is believed that the cancerous cells produce higher amounts of ROS than normal cells via increased metabolic rate and relative hypoxia. The selective cytotoxicity values of Ag–Cu NPs were 12.25 and 24.75 for PC-3 and LNCaP compared to HEK293, respectively. The calculated selectivity for cancer cells was 2.02 which indicated the more toxicity of the NPs against LNCaP cells. These two cell lines are widely used as cell models of low and high metastatic potential. The obtained IC50 values were subsequently used for apoptosis testing (flow cytometry), gene expression analysis, and assessment of reactive oxygen species (ROS) production.

Table 2: Half-maximal inhibitory concentration percentage (µg/ml) of the treatments used in the current study

Cell lines	Treatments	24 h	48 h	72 h
HEK-293	Ag–Cu NPs	136.3	293.2	137.6
	Extract	208.4	232.9	131
PC3	Ag–Cu NPs	16.39	15.95	13.94
	Extract	29.59	17.58	17.13
LNCaP	Ag–Cu NPs	9.945	6.531	6.437
	Extract	20.44	10.41	9.88

Real-time PCR

The gene expression profiles of exposed PC-3 and LNCaP exposed cells to Ag–Cu NPs and plant extract are presented in Figure 4a and b. *VEGF* mRNA, the angiogenesis inducer, significantly decreased by both treatments in both cell lines treated with biogenic NPs ($P < 0.01$ and $P < 0.001$ for PC-3 and LNCaP, respectively). The inhibiting *VEGF* expression activity of the herbal extract was not significant in both extract-treated cell lines. In our project, in both cell lines, biogenic NPs reduced *MMP2* and *MMP9* mRNA levels by up to half of their expression in the control group. A total of 0.8-fold change was observed after the exposure to the plant extract. As it was predictable, NPs had a more pronounced effect on the reduction of *MMP9* gene expression compared to the plant extract. Also, NPs were more effective on the LNCaP cell line by reducing *MMP9* expression. For the *MMP2* gene,

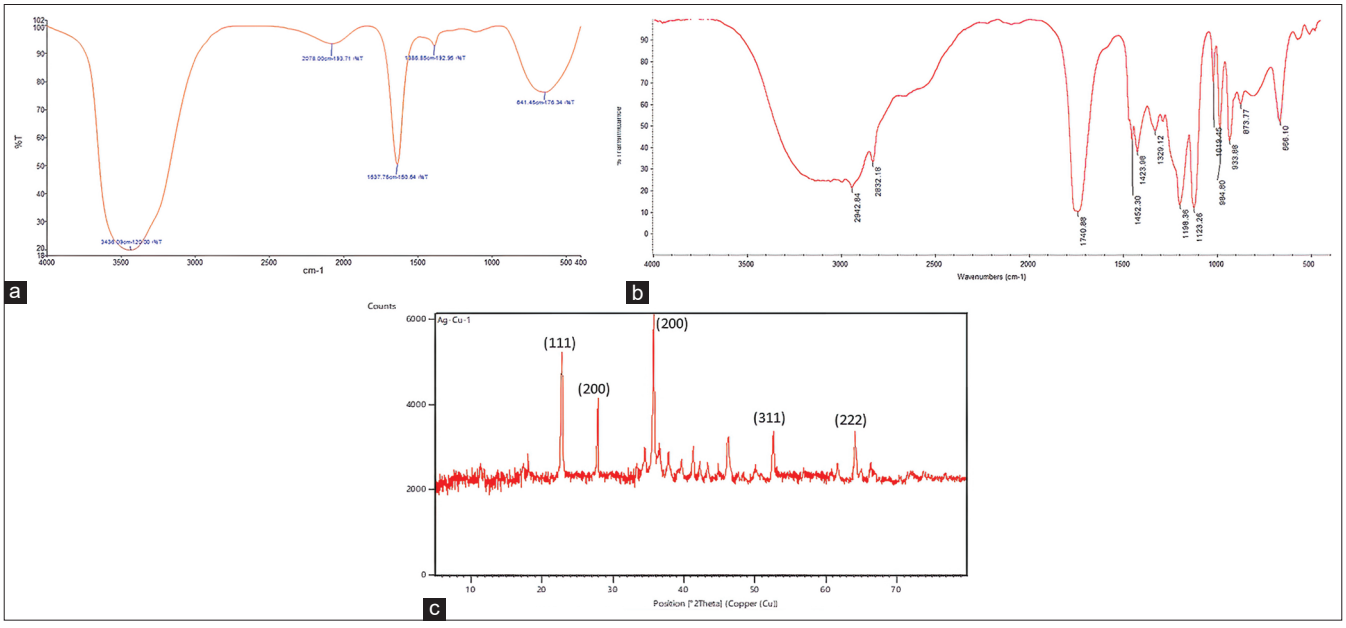

Figure 2: FT-IR spectrum of (a) Extract, and (b) Ag–Cu NPs, and (c) XRD graph of Ag–Cu NPs

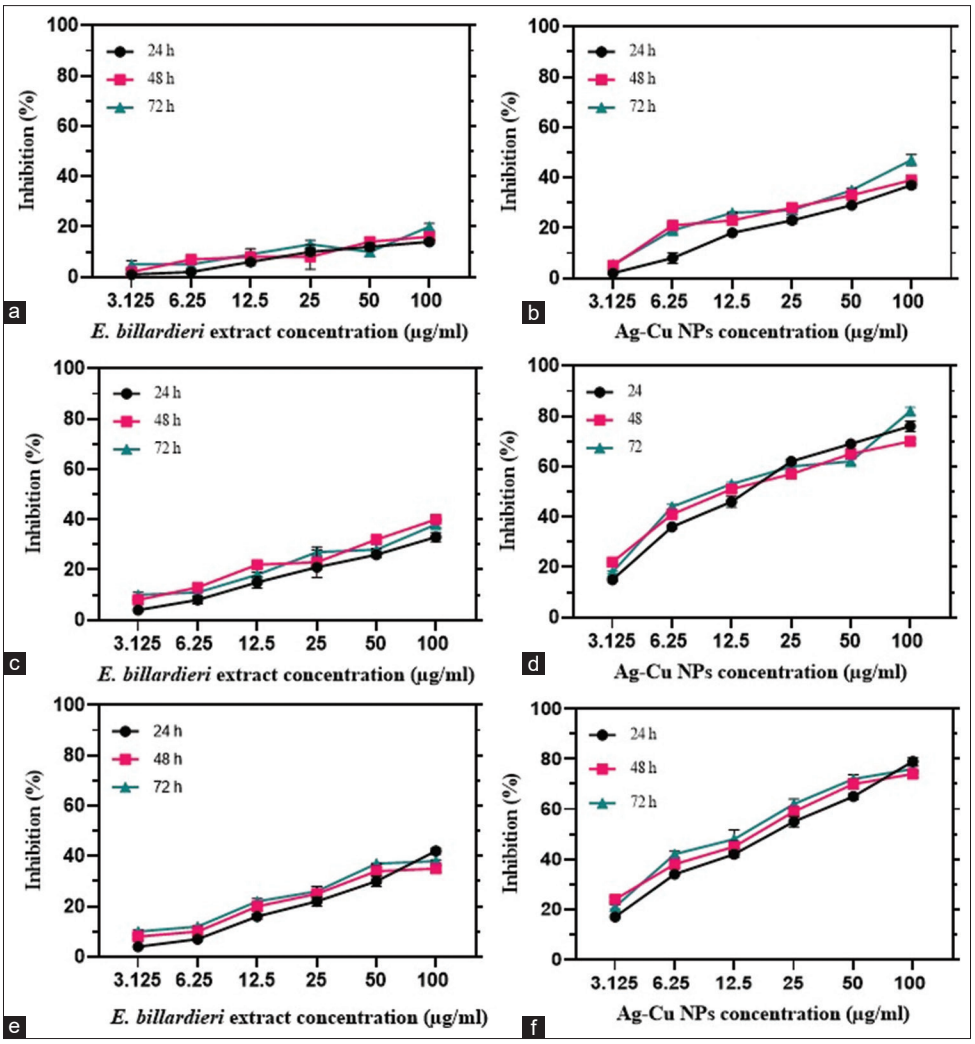

Figure 3: *In vitro* cytotoxicity of *E. billardieri* extract and Ag-Cu NPs. MTT assay results for HEK-293, PC-3, and LNCaP treated with *E. billardieri* for 24, 48, and 72 h (a, c, and e). MTT assay results for HEK-293, PC-3, and LNCaP treated with Ag–Cu NPs for 24, 48, and 72 h (b, d, and f)

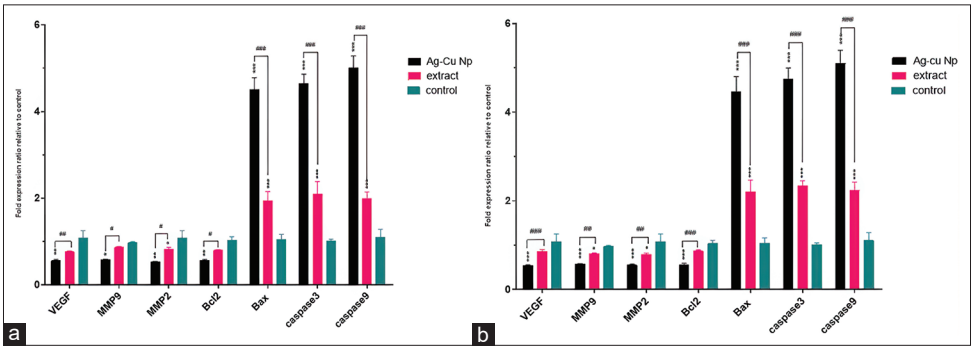

Figure 4: *Bax*, *Bcl2*, *caspase3*, *caspase3*, *VEGF*, *MMP2*, and *MMP9* expression levels in (a) PC-3, (b) LNCaP cell lines treated with IC50 concentration of extract as well as Ag–Cu NPs after 24 h. (*:$P < 0.05$, **:$P < 0.01$, ***:$P < 0.001$, and ****:$P < 0.0001$)

the reducing trend of NPs on *MMP2* expression was similar to *MMP9*. It is noteworthy to mention that the biogenic NP effects were higher against *MMP2* in comparison to *MMP9,* while the effect of the extract was the same. Although the extract caused a reduction in *Bcl2* expression, it could not be statistically considered significant. Bax is a pro-apoptotic effector. The Ag–Cu NPs exposure increased *Bax* mRNA levels to 4.5 and 4.3-fold in PC-3 and LNCaP, respectively. While our plant extract was compatible with increasing the expression of *Bax* around two-fold, it was not as effective as the NP. The changes in the expression of *Bcl2* and *Bax* can be considered a relatively apoptotic induction ability of biogenic Ag–Cu by

E. billardieri. Current results support the pro-apoptotic ratio of *Bax* and *Bcl2* in mRNA levels. Both plant extract and Ag–Cu NPs prompted the rise in *caspase-3* and *caspase-9* expression; however, NPs showed a more profound effect on both cell lines. The NPs had a more pronounced effect on the increase of *caspase3* gene expression compared to the plant extract, with statistically significant differences at $P < 0.001$ and $P < 0.05$.

Flow cytometry results

For a more detailed investigation of cellular death (apoptosis or necrosis), an Annexin V-PI and flow cytometry analysis were employed. In Figure 5a, the results of cell staining for PC-3 cells are presented. Flow cytometry results in the conducted research indicate that in the control cells, which were not subjected to treatment, around 98% of the cells remained alive. This is expected as most of the control cells are not expected to undergo apoptosis since they were neither treated with NPs nor the herbal extract. The percentage of cells undergoing early apoptosis is 3%, while 0% of the cells underwent late apoptosis, and a minimal amount of 0.4% of the cells underwent necrosis. According to the results obtained at the IC50 concentration of the herbal extract and silver–copperNPs, the percentage of live cells (Q4 region) was 85% and 68%, respectively. The percentage of cells undergoing early apoptosis (Q3 region) was 5% and 14%, and the cells undergoing late apoptosis (Q2 region) were approximately 8% and more than 10%, respectively. Additionally, the percentage of necrotic cells (Q1 region) in response to the IC50 concentration of the herbal extract, silver, and copper NPs was 2.5% and 8%, respectively [Figure 5a]. The diagram illustrates that the percentage of cells exposed to NPs has a significantly higher occurrence of early apoptosis compared to other groups [Figure 5b]. Additionally, the percentage of cells undergoing late apoptosis in NPs-exposed cells is statistically higher than in other groups. However, it can be observed that the level of early apoptosis is higher than late apoptosis in NPs-exposed cells. The percentage of late apoptosis in cells treated with the herbal extract is higher than early apoptosis, and all mentioned *P* -values are significant ($P < 0.001$). The percentage of early apoptosis, late apoptosis, and necrosis were estimated at 10%, 14%, and 12% for Ag–Cu NPs treatment and 4.5%, 8%, and 4% for extract in LNCaP cells, respectively [Figure 5c]. The apoptosis rate in extract-treated LNCaP cells was lower than in Ag–Cu NPs-treated cells [Figure 5d]. Intriguingly, the exposure to the plant extract did not act differently on the cell lines and the rates of apoptosis were similar. However, the difference observed in the distribution of PC-3 and LNCaP cell lines, suggests different responses to the NP treatment.

ROS analysis

ROS or reactive oxygen species are highly reactive molecules and free radicals derived from oxygen molecules. Many studies have revealed that ROS play a significant part in the inhibitory behavior of tumor-induced immunosuppressive cells. As shown in Figure 6, our derived biosynthesized bimetallic NPs generated ROS more efficiently than the plant extract in 24 h exposure. As demonstrated in Figure 6a and b, approximately 1.5-fold and 1.6-fold enhancement was observed in the ROS content of PC-3and LNCaP cells after treatment with extract

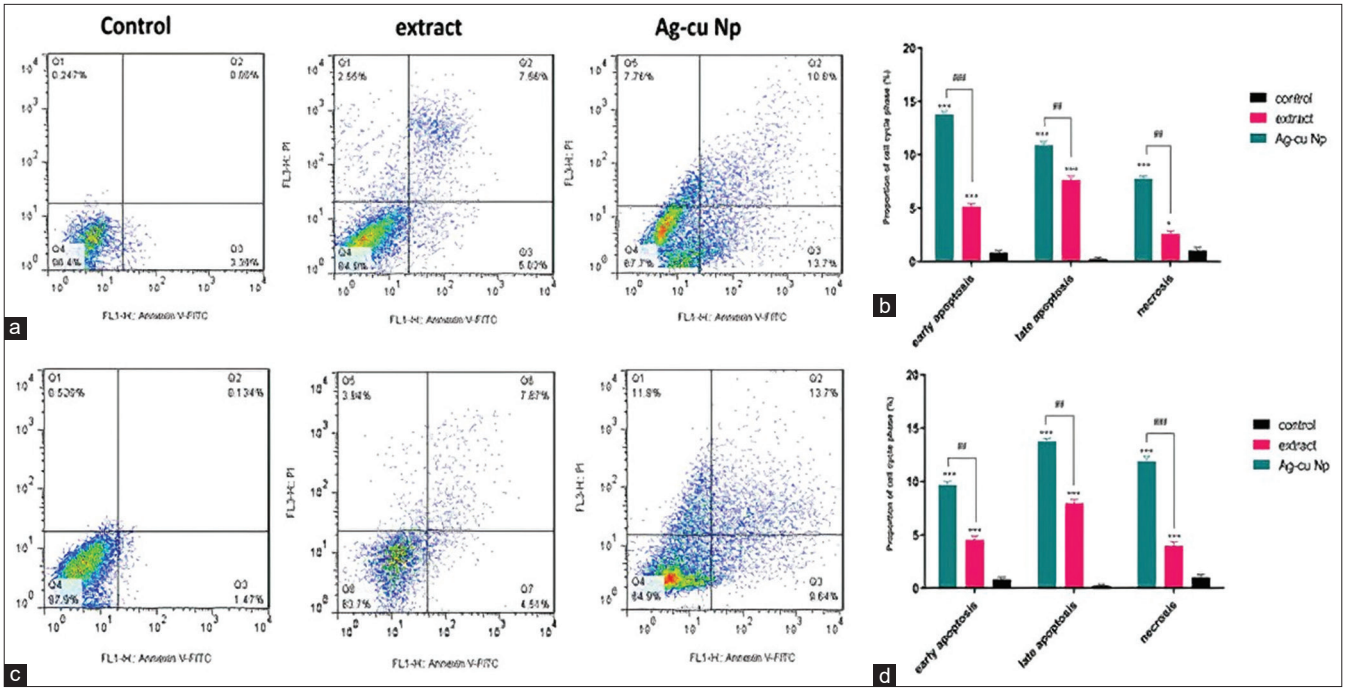

Figure 5: Apoptosis rate in (a) PC-3, (c) LNCaP cells treated with IC50 concentrations of Ag–Cu NPs. (b, d) Comparison of apoptosis and necrosis rate in (b) PC-3, (d) LNCaP cells treated with IC50 concentrations of the extract as well as Ag–Cu NPs after 24 h treatment. (*:$P < 0.05$, ****:$P < 0.0001$, ##:$P < 0.01$, ###:$P < 0.001$)

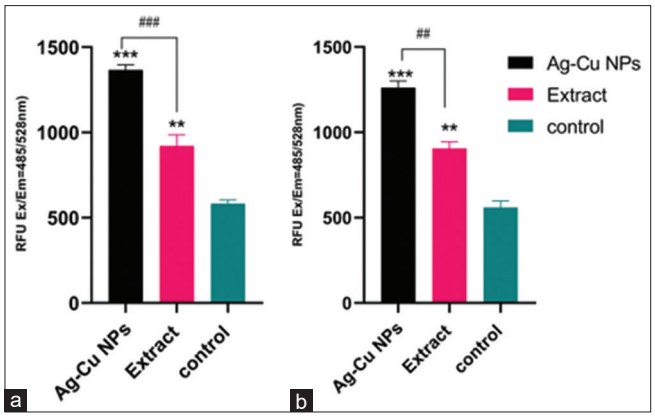

Figure 6: ROS levels in (a) PC-3, (b) LNCaP cell lines treated with IC50 concentration of the extract and Ag–Cu NPs after 24 h (*:$P < 0.05$, and, ***:$P < 0.001$)

the 24 h treatment, compared to the control and 2.3-fold and 2.4-fold enhancement after treatment with Ag–Cu NPs compared to the control, respectively.

Discussion

E. billardieri belongs to the *Apiaceae* family, growing worldwide. Its richness of phytoconstituents, such as saponins, phenolic acids, and flavonoids, has held it as a considerable medicinal herb since ancient times. Also, a recent biological assessment has revealed its potential anticancer pharmaceutical features.[26–28] In this research, *E. billardieri* aqueous leaf extract's functional phytoconstituents interacted with synthesized nanostructures, and the produced Ag–Cu microstructure showed a smooth surface.[29] Ag–Cu NP TEM micrographs, which appeared to have an uneven distribution, are shown to have a high magnification in the results.[30] The extracts' increasing levels of phenolic and other phytochemical constituents were the direct cause of the agglomerated nanomaterials.[31] According to certain earlier studies, the reduction of metal cations into metal NPs may be due to the hydroxyl (-OH) moieties present in flavonoids.[32,33] It is plausible that flavonoids' keto-enol transformation from the = C-OH to the C = O form may release extremely reactive hydride ions, which transform $CuSO_4$ into Cu nanocomposites and reduce Ag+ to Ag0 NPs. To stop further growth and accumulation, stabilizing the NPs is the second important function of capping phytochemicals following metal reduction. The phytochemicals' hydrophobic polyaromatic cyclic skeleton provides steric hindrance to prevent NP agglomeration and stabilizes the resulting nanocomposites, while the hydrophilic points (-OH, -NH, -O–) interact with Ag and Cu metal ions.[34] The plant extract dramatically lowers and stabilizes metal ions due to the presence of multiple active biomolecules with different functional groups. Another possibility is that Ag+ acts like a Lewis acid, taking electrons from the phytocompounds' active Lewis bases, forming π-bonded complexes with polyaromatic cyclic skeletons. However, due to the wide range of phytochemicals present in the herbal extract, it is difficult to pinpoint the exact reducing and stabilizing agents for the synthesis of NPs.

Our cytotoxic results indicated good biocompatibility of the biogenic NPs to normal cells, besides their high anticancer effects against two different PC cell lines. Previous studies on *E. billardieri* extract and biogenic synthesized Ag NPs by *E. billardieri* also reached similar results to us.[26,35] *E. billardieri* has been frequently used as antidiabetic herbal medicine since ancient times. It has been known that the chemical compounds, reducing glucose uptake or glucose metabolism in cells, positively impact normal cell survival and may have potential anticancer properties.[36] Our MTT results are in accordance with it. Therefore, it can be concluded that *E. billardieeri*-originated Ag–Cu NPs had anticancer characteristics. In a study conducted by Ramadi *et al*.,[37] they found that Ag–Cu NP's concentration above 20 µg/mL is toxic in healthy cells. The toxicity of our biogenic Ag–Cu NPs against normal cells was relatively less than their study, which could be due to the phytoconstituents of *E. billardieri*.

As the results present the biogenic NPs were more influential on cancerous cells than the extract. It is believed that the cancerous cells produce higher amounts of ROS than normal cells via increased metabolic rate and relative hypoxia. However, these cells orchestrate mechanisms to minimize ROS adverse effects, such as activating antiapoptotic pathways and upregulating antioxidant defense.[38] These altered modulation of cellular defense in front of ROS, make them a proper target for NPs, which was demonstrated by former studies using Ag–Cu NPs.[22,35] The selective cytotoxicity values of Ag–Cu NPs were 12.25 and 24.75 for PC-3 and LNCaP compared to HEK293, respectively. The calculated selectivity for cancer cells was 2.02 which indicated the greater toxicity of the NPs against LNCaP cells. These two cell lines are widely used as cell models of low and high metastatic potential. Dozmorov *et al*.[39] found the difference between molecular profiles of LNCaP and PC-3. These differences can lead to the divergent responses of LNCaP and PC-3 to Ag–Cu NPS, which are related to metabolic and uptake mechanisms as well as cytoskeleton genes and different androgen sensitivity.

VEGF, the angiogenesis inducer, indirectly suppresses cell death. In our study, *VEGF* mRNA significantly decreased by NPs in both cell lines. Research has demonstrated that VEGF can prevent cancer cells from dying due to providing a nutrient supply for cancerous cells.[40] *VEGF* overexpression in PC is associated with poor prognosis, cancer progression, and metastasis. Ongoing investigations demonstrate the promising application of antiangiogenic agents in PC treatment.[41] Based on our knowledge, there is no other study on green-synthesized Ag–Cu NPs investigating the *VEGF* gene expression.

Matrix metalloproteinases (MMPs) are enzymes that break down the extracellular matrix's constituent parts. *MMP9* and *MMP2* are examples of MMPs. *MMP2* and *MMP9* are linked to the invasion and metastasis of the tumor. Collagen types IV and V, which make up the majority of the basement membrane, are

known to be broken down by MMP9. Tumor cell invasion of surrounding tissues and blood vessels is facilitated by MMPs' degradation of the basement membrane. Type IV collagen, an important part of the basement membrane, is mainly broken down by MMP2. Like MMP9, MMP2 encourages the migration of tumor cells into the surrounding tissues and blood vessels and aids in the disruption of the basement membrane.[42] It is noteworthy that one of the most important aspects of managing tumor invasion and metastasis is the regulation of MMP activity. In our study, the mRNA levels of both MMP2 and 9 were reduced dramatically. However, in a previous report on Ag–Cu NPs and the expression of MMP2 and 9 protein levels in breast cancer, the upregulation of MMP9 was observed, while the expression of MMP2 protein remains unaffected.[22] The results of their study were not in line with our study. It could be due to the different doses of Ag–Cu NPs and the different ratios of silver and copper in the composite NPs. Besides, the way used for NP synthesis must not be excluded, because the green synthesized NPs can carry the active components of the herbal extract, which can synergistically boost the anticancer properties of NPs.[39]

Bax and *Bcl2* are proteins that have a pivotal role in the control of apoptosis. According to research, Ag–Cu NPs can influence the levels of *Bax* and *Bcl2* in cancer cells. Various studies conducted on Ag–NPs and Cu-NPs indicated their roles in apoptosis induction.[43–45] Our results revealed that the composite of silver and copper on the nanoscale saves the proapoptotic characteristics of both elements. *Bcl2* is an antiapoptotic protein in cells. It inhibits the release of cytochrome C from mitochondria, which is a critical step in the activation of apoptosis. *Bcl2* is known to enhance cell survival and is aberrantly overexpressed in cancer cells, adding to their apoptosis resistance.[46] In contrast, *Bax* is a pro-apoptotic protein promoting cell death. It opens various holes in the outer mitochondrial membrane, allowing cytochrome C to be released and downstream apoptotic pathways to be activated. *Bax* regulates apoptosis in a variety of settings, including normal development and illness.[47] The expression ratio of *Bax* to *Bcl2* is thought to be a crucial determinant of cell fate in response to apoptotic stimuli. A higher *Bax*/*Bcl2* ratio promotes apoptosis, whereas a lower ratio supports cell survival. This ratio works as a cell death switch, shifting the balance between cell survival and cell death.[48,49] The observed changes in the expression of *Bcl2* and *Bax* can be considered a relatively apoptotic inducive ability of biogenic Ag–Cu by *E. billardieri*. In our study, both NPs and herbal extract increased the mRNA expression of caspases. Caspases play essential role in orchestrating apoptosis. They are a distinct family of cysteine proteases that reside in cells as dormant zymogens and are activated during apoptosis.[42] Activation of apoptotic caspases causes substrates to be inactivated or activated, resulting in a cascade of signaling events and cell death. In addition to their involvement in apoptosis, caspases have been found to have non-apoptotic roles in cellular proliferation and disease processes.[50,51] These other forms of cell death include necroptosis, pyroptosis, and autophagy.[52] Particularly significant during the apoptotic execution phase are *caspases-3* and *caspase-9*. Caspase-9 is the crucial initiator of the mitochondrial (i.e., intrinsic) apoptosis pathway. Activated caspase-9 cleaves caspase-3 which is a key player in the execution phase of apoptosis. Once caspase-3 is cleaved by caspase-9, it drives major events in apoptosis which leads to the morphological hallmarks of apoptosis. It has been documented that silver and copper NPs induced apoptosis through the production of ROS. The increase of ROS production in cells triggers the intrinsic apoptosis pathway in which both caspase-9 and caspase-3 are involved,[53–55] this pattern has been replicated in the current investigation.

LNCaP presented a higher rate of late apoptosis and necrosis than early apoptosis. It could be interpreted that these cells tend to have a slower apoptotic response to Ag–Cu NPs than PC-3. Also, it can result from other cell death pathways activated through the treatment. PC-3 showed a higher rate of early apoptosis to necrosis and late apoptosis, which may suggest that it rapidly undergoes apoptosis after Ag–Cu NPs exposure. Additionally, a lower percentage of cells in late apoptosis and necrosis can show a more efficient apoptotic response compared to LNCaP. These observed variations in response to biogenic NPS could be related to differences in genetics and activated signaling pathways of LNCaP and PC-3.

In a study conducted by Al Tamimi *et al*.,[22] the researchers showcased the specific toxicity of Ag/Cu-NP alloy toward MCF7 cells, which are breast cancer cellular models. Their findings revealed no discernible staining in either early or late apoptosis, but the number of necrotic cells rose by 20%. They proposed that the cell death pathway might be involved in other mechanisms. They also used an apoptosis assay in lung cancer NCI-1975 cells to demonstrate the toxic effect of Ag–Cu NP, and the results showed a significant difference in the early and late apoptosis stages when compared to the control group. Additionally, the toxicity may involve various pathways for cell death in various cancer cell types.

ROS are synthetically responsive atoms that contain oxygen and are created because of typical cell digestion. ROS plays a critical part in different cell processes, including cell flagging and resistant reactions. Be that as it may, unnecessary ROS creation can prompt oxidative pressure, harming cell parts like DNA, proteins, and lipids. The anticancer potential of silver and copper in combination with various medicinal plant extracts has been reported in prostate cancer.[56–58] For instance, in a study conducted by Zhang, the *Salvia miltiorrhiza*-derived Ag NPs induced cytotoxicity, apoptosis, and oxidative stress through the modulation of intrinsic apoptotic *Bax*, *BCL2*, and *Caspase-3* mRNA expression in LNCaP cell line.[54] In another study, Bai *et al*.[59] used *Acroptilon repens* leaf extract to green synthesize Cu NPs and examined its anticancer effects on lung cancer cell lines. Their results showed an increased induction of apoptosis and ROS production due to biogenic Cu NPs. Comparing the results of NPs' treatment in PC-3 to

LNCaP demonstrated a not statistically significant difference in ROS production, which probably showed the importance of molecular pathways involved in the production of ROS.

Silver and copper NPs predominantly enter cells via endocytosis. In the cells, silver interacts with cellular compounds leading to adverse effects on cellular mechanisms by which inducing ROS production. On the other side, copper is a component of many enzymes and transcription factors; however, it can increase cellular toxicity and programmed cell death through different mechanisms one is ROS production. The consequence of excessive ROS production is oxidative stress which triggers the activation of pro-apoptotic molecules (e.g., BAX) and inhibition of antiapoptotic ones (e.g., BCL2).[60,61] Our real-time PCR and flow cytometry results were in accordance with the increase of ROS, suggesting the anticancer potential of *E. billardieri* biogenic Ag–Cu NPs can be investigated more in future studies.

Despite all the advantages mentioned for biogenic Ag–Cu NPs, there are many challenges for the clinical use.[62] For example, it can be said that the presence of these NPs as a treatment for PC may reduce sperm motility and quality.[63] As sperm quality plays a crucial role in fertility[64], it seems that investigating the effect of these NPs on sperm can be a suitable approach to evaluate the clinical application of theseNPs.[65]

Considering the electrical conductivity and ionic nature of the resulting NPs, it seems that their combination with biophysical variables such as electric or magnetic fields can improve the performance of NPs.[66,67] Also, due to the ability of metal NPs to bind to proteins and enzymes, it is possible to use them in targeted treatment for PC.[68]

Conclusion

The Ag–Cu NPs were effectively orchestrated through a naturally harmless methodology by utilizing a watery leaf extract of *E. billardieri* plant and were considered for their anticancer action against PC-3 and LNCaP prostate malignant cell lines. Portrayal methods like XRD, SEM, EDAX, FTIR, and SEM studies have affirmed the development of integrated NPs. Moreover, the anticancer effects of Ag-Cu NPs were examined against human prostate PC-3 and LNCaP cells which showed it as an apoptotic inducer and anti-metastatic nanocomposite. It seems that increased levels of ROS brought about this observation.

Ethics approval and consent to participate

There are no “human subjects” in this study

Acknowledgments

The authors would like to acknowledge the Central Tehran Branch, Islamic Azad University for providing the necessary laboratory facilities for this study.

Financial support and sponsorship

Nil.

Conflicts of interest

There are no conflicts of interest.

References

1. Sekhoacha M, Riet K, Motloung P, Gumenku L, Adegoke A, Mashele S. Prostate cancer review: Genetics, diagnosis, treatment options, and alternative approaches. Molecules 2022;27:5730.
2. Ashrafizadeh M, Aghamiri S, Tan SC, Zarrabi A, Sharifi E, Rabiee N, *et al*. Nanotechnological approaches in prostate cancer therapy: Integration of engineering and biology. Nano Today 2022;45:101532.
3. Patel JK, Patel AP. Passive targeting of nanoparticles to cancer. In: Pathak Y, editor. Surface Modification of Nanoparticles for Targeted Drug Delivery. Cham: Springer; 2019. p. 125–43.
4. Sun W, Deng Y, Zhao M, Jiang Y, Gou J, Wang Y, *et al*. Targeting therapy for prostate cancer by pharmaceutical and clinical pharmaceutical strategies. J Control Release 2021;333:41–64.
5. Peng ZH, Sima M, Salama ME, Kopečková P, Kopeček J. Spacer length impacts the efficacy of targeted docetaxel conjugates in prostate-specific membrane antigen expressing prostate cancer. J Drug Target 2013;21:968–80.
6. Gavas S, Quazi S, Karpiński TM. Nanoparticles for cancer therapy: Current progress and challenges. Nanoscale Res Lett 2021;16:173.
7. He Y, Du Z, Ma S, Cheng S, Jiang S, Liu Y, *et al*. Biosynthesis, antibacterial activity and anticancer effects against prostate cancer (PC-3) cells of silver nanoparticles using Dimocarpus Longan Lour. peel extract. Nanoscale Res Lett 2016;11:1–10.
8. Biresaw SS, Taneja P. Copper nanoparticles green synthesis and characterization as anticancer potential in breast cancer cells (MCF7) derived from Prunus nepalensis phytochemicals. Mater Today Proc 2022;49:3501–9.
9. Nicolae-Maranciuc A, Chicea D, Chicea LM. Ag Nanoparticles for biomedical applications—Synthesis and characterization—A Review. Int J Mol Sci 2022;23:5778.
10. Jafari A, Niknam Z, Rahimi M, Zali H, Rezaei-Tavirani M. Silver nanoparticles inhibit proliferation and migration of prostate cancer cells: An experimental report. World Cancer Res J 2022;9:e2242.
11. El-Magid ADA, AbdEl-Hamid OM, Younes MA. The biochemical effects of silver nanoparticles and spirulina extract on experimentally induced prostatic cancer in rats. Biol Trace Elem Res 2023;201:1935–45.
12. Takáč P, Michalková R, Čižmáriková M, Bedlovičová Z, Balážová Ľ, Takáčová G. The role of silver nanoparticles in the diagnosis and treatment of cancer: Are there any perspectives for the future? Life (Basel) 2023;13:466.
13. Šulce A, Bulke F, Schowalter M, Rosenauer A, Dringen R, Kunz S. Reactive oxygen species (ROS) formation ability and stability of small copper (Cu) nanoparticles (NPs). RSC Adv 2016;6:76980–8.
14. Aishajiang R, Liu Z, Wang T, Zhou L, Yu D. Recent advances in cancer therapeutic copper-based nanomaterials for antitumor therapy. Molecules 2023;28:2303.
15. Ji P, Wang P, Chen H, Xu Y, Ge J, Tian Z, *et al*. Potential of copper and copper compounds for anticancer applications. Pharmaceuticals (Basel) 2023;16:234.
16. Shaaban MT, Mohamed BS, Zayed M, El-Sabbagh SM. Antibacterial, antibiofilm, and anticancer activity of silver-nanoparticles synthesized from the cell-filtrate of Streptomyces enissocaesilis. BMC Biotechnol 2024;24:8.
17. Andleeb A, Andleeb A, Asghar S, Zaman G, Tariq M, Mehmood A, *et al*. A systematic review of biosynthesized metallic nanoparticles as a promising anti-cancer-strategy. Cancers (Basel) 2021;13:2818.
18. Thirumoorthy G, Balasubramanian B, George JA, Nizam A, Nagella P, Srinatha N, *et al*. Phytofabricated bimetallic synthesis of silver-copper nanoparticles using Aerva lanata extract to evaluate their potential cytotoxic and antimicrobial activities. Sci Rep 2024;14:1270.
19. Tao Y, Zhou F, Wang K, Yang D, Sacher E. AgCu NP Formation by the Ag NP Catalysis of Cu ions at room temperature and their antibacterial efficacy: A kinetic study. Molecules 2022;27:6951.

20. Ahmad M, Nawaz T, Assiri MA, Hussain R, Hussain I, Imran M, *et al*. Fabrication of bimetallic Cu-Ag nanoparticle-decorated poly (cyclotriphosphazene-co-4,4′-sulfonyldiphenol) and its enhanced catalytic activity for the reduction of 4-nitrophenol. ACS Omega 2022;7:7096–102.
21. Malik MA, Albeladi SS, Al-Maaqar SM, Alshehri AA, Al-Thabaiti SA, Khan I, *et al*. Biosynthesis of novel Ag-Cu bimetallic nanoparticles from leaf extract of Salvia officinalis and their antibacterial activity. Life 2023;13:653.
22. Al Tamimi S, Ashraf S, Abdulrehman T, Parray A, Mansour SA, Haik Y, *et al*. Synthesis and analysis of silver–copper alloy nanoparticles of different ratios manifest anticancer activity in breast cancer cells. Cancer Nanotechnol 2020;11:13.
23. Vaid P, Raizada P, Saini AK, Saini RV. Biogenic silver, gold and copper nanoparticles-A sustainable green chemistry approach for cancer therapy. Sustain Chem Pharm 2020;16:100247.
24. Hussain I, Singh NB, Singh A, Singh H, Singh SC. Green synthesis of nanoparticles and its potential application. Biotechnol Lett 2016;38:545–60.
25. Chamgordani ZH, Mazaheri M, Iraj B, Baghshahi H, Sabouhi F. Antidiabetic effects of Eryngium billardieri hydrosol in the treatment of type 2 diabetic patients: A double-blind randomized clinical trial. Avicenna J Phytomed 2023;13:34–44.
26. Roshanravan N, Asgharian P, Dariushnejad H, Alamdari NM, Mansoori B, Mohammadi A, *et al*. Eryngium billardieri induces apoptosis via BAX gene expression in pancreatic cancer cells. Adv Pharm Bull 2018;8:667–74.
27. Hasanbeiglu S, Hosseini K, Molavi O, Asgharian P, Tarhriz V. Eryngium billardieri extract and fractions induce apoptosis in cancerous cells. Anticancer Agents Med Chem 2021;22:2189–201.
28. Daneshzadeh MS, Abbaspour H, Amjad L, Nafchi AM. An investigation on phytochemical, antioxidant and antibacterial properties of extract from Eryngium billardieri F. Delaroche. J Food Meas Charact 2020;14:708–15.
29. Karekar N, Karan A, Khezerlou E, Prajapati N, Pernici CD, Murray TA, *et al*. Self-assembled metal–organic biohybrids (MOBs) using copper and silver for cell studies. Nanomaterials 2019;9:1282.
30. Huang J, Guo J, Zhu J, Zou X. Supported silver nanoparticles over alginate-modified magnetic nanoparticles: Synthesis, characterization and treat the human lung carcinoma. J Saudi Chem Soc 2022;26:101393.
31. Abdellatif AAH, Abdelfattah A, Bouazzaoui A, Osman SK, Al-Moraya IS, Showail AMS, *et al*. Silver nanoparticles stabilized by poly (vinyl pyrrolidone) with potential anticancer activity towards prostate cancer. Bioinorg Chem Appl 2022;2022:6181448.
32. El-Seedi HR, El-Shabasy RM, Khalifa SAM, Saeed A, Shah A, Shah R, *et al*. Metal nanoparticles fabricated by green chemistry using natural extracts: Biosynthesis, mechanisms, and applications. RSC Adv 2019;9:24539–59.
33. Sierra JA, Vanoni CR, Tumelero MA, Cid CCP, Faccio R, Franceschini DF, *et al*. Biogenic approaches using citrus extracts for the synthesis of metal nanoparticles: The role of flavonoids in gold reduction and stabilization. New J Chem 2016;40:1420–9.
34. Abu El-Soad AMA. Novel adsorbents based on chitosan and halloysite nanotubes for sorption of Cu (II) and Zn (II) metal ions: Dissertation for a degree candidate of chemical sciences: 1.4. 4. б. и 2023.
35. Allafchian A, Balali F, Reza Vahabi M, Amir Hossein Jalali S. Antibacterial and cytotoxic effects of silver nanoparticles fabricated by Eryngium billarderi Delar. Extract. Chem Phys Lett 2022;791:139385.
36. Talib WH, Mahmod AI, Abuarab SF, Hasen E, Munaim AA, Haif SK, *et al*. Diabetes and cancer: Metabolic association, therapeutic challenges, and the role of natural products. Molecules 2021;26:2179.
37. Ramadi KB, Mohamed YA, Al-Sbiei A, Almarzooqi S, Bashir G, Al Dhanhani A, *et al*. Acute systemic exposure to silver-based nanoparticles induces hepatotoxicity and NLRP3-dependent inflammation. Nanotoxicology 2016;10:1061–74.
38. Singh R, Manna PP. Reactive oxygen species in cancer progression and its role in therapeutics. Explor Med 2022;3:43–57.
39. Dozmorov MG, Hurst RE, Culkin DJ, Kropp BP, Frank MB, Osban J, *et al*. Unique patterns of molecular profiling between human prostate cancer LNCaP and PC-3 cells. Prostate 2009;69:1077–90.
40. Duffy AM, Bouchier-Hayes DJ, Harmey JH. Vascular endothelial growth factor (VEGF) and its role in non-endothelial cells: Autocrine signalling by VEGF. In: Madame Curie Bioscience Database. Landes Bioscience; 2013.
41. Melegh Z, Oltean S. Targeting angiogenesis in prostate cancer. Int J Mol Sci 2019;20:2676.
42. Zheng H, Takahashi H, Murai Y, Cui Z, Nomoto K, Niwa H, *et al*. Expressions of MMP-2, MMP-9 and VEGF are closely linked to growth, invasion, metastasis and angiogenesis of gastric carcinoma. Anticancer Res 2006;26:3579–83.
43. Dolati M, Tafvizi F, Salehipour M, Komeili Movahed T, Jafari P. Biogenic copper oxide nanoparticles from Bacillus coagulans induced reactive oxygen species generation and apoptotic and anti-metastatic activities in breast cancer cells. Sci Rep 2023;13:3256.
44. Plackal Adimuriyil George B, Kumar N, Abrahamse H, Ray SS. Apoptotic efficacy of multifaceted biosynthesized silver nanoparticles on human adenocarcinoma cells. Sci Rep 2018;8:14368.
45. Daei S, Ziamajidi N, Abbasalipourkabir R, Aminzadeh Z, Vahabirad M. Silver nanoparticles exert apoptotic activity in bladder cancer 5637 cells through alteration of Bax/Bcl-2 genes expression. Chonnam Med J 2022;58:102-9.
46. Kulsoom B, Shamsi TS, Afsar NA, Memon Z, Ahmed N, Hasnain SN. Bax, Bcl-2, and Bax/Bcl-2 as prognostic markers in acute myeloid leukemia: Are we ready for Bcl-2-directed therapy? Cancer Manag Res 2018;10:403–16.
47. Guo B, Zhai D, Cabezas E, Welsh K, Nouraini S, Satterthwait AC, *et al*. Humanin peptide suppresses apoptosis by interfering with Bax activation. Nature 2003;423:456–61.
48. Misao J, Hayakawa Y, Ohno M, Kato S, Fujiwara T, Fujiwara H. Expression of bcl-2 protein, an inhibitor of apoptosis, and Bax, an accelerator of apoptosis, in ventricular myocytes of human hearts with myocardial infarction. Circulation 1996;94:1506–12.
49. Niu G, Gao F, Wang Y, Zhang J, Zhao L, Jiang Y. Bimetallic nanomaterials: A promising nanoplatform for multimodal cancer therapy. Molecules 2022;27:8712.
50. Kasravi M, Yaghoobi A, Tayebi T, Hojabri M, Taheri AT, Shirzad F, *et al*. MMP inhibition as a novel strategy for extracellular matrix preservation during whole liver decellularization. Biomater Adv 2024;156:213710.
51. Jiang H, Li H. Prognostic values of tumoral MMP2 and MMP9 overexpression in breast cancer: A systematic review and meta-analysis. BMC Cancer 2021;21:1–13.
52. Sahoo G, Samal D, Khandayataray P, Murthy MK. A review on caspases: Key regulators of biological activities and apoptosis. Mol Neurobiol 2023;60:5805–37.
53. Bao J, Jiang Z, Ding W, Cao Y, Yang L, Liu J. Silver nanoparticles induce mitochondria-dependent apoptosis and late non-canonical autophagy in HT-29 colon cancer cells. Nanotechnol Rev 2022;11:1911–26.
54. Tang J, Lu X, Chen B, Cai E, Liu W, Jiang J, *et al*. Mechanisms of silver nanoparticles-induced cytotoxicity and apoptosis in rat tracheal epithelial cells. J Toxicol Sci 2019;44:155–65.
55. Wang T, Wen X, Hu Y, Zhang X, Wang D, Yin S. Copper nanoparticles induced oxidation stress, cell apoptosis and immune response in the liver of juvenile Takifugu fasciatus. Fish Shellfish Immunol 2019;84:648–55.
56. Jabeen S, Qureshi R, Munazir M, Maqsood M, Munir M, Shah SSH, *et al*. Application of green synthesized silver nanoparticles in cancer treatment-A critical review. Mater Res Express 2021;8:092001.
57. Goel A, Bhatia AK. Phytosynthesized nanoparticles for effective cancer treatment: A Review. Nanosci Nanotechnology-Asia 2018;9:437–43.
58. Elbagory AM, Hull R, Meyer M, Dlamini Z. Reports of plant-derived nanoparticles for prostate cancer therapy. Plants (Basel) 2023;12:1870.
59. Bai X, Tang J, Safaralizadeh R, Feizi MAH, Delirezh N, Zangeneh A, *et al*. Green fabrication of bioactive copper nanoparticles using Acroptilon repens extract: An enhanced anti-lung cancer activity. Inorg Chem Commun 2024;164:112393.
60. Lee MJ, Lee SJ, Yun SJ, Jang JY, Kang H, Kim K, *et al*. Silver nanoparticles affect glucose metabolism in hepatoma cells through production of reactive oxygen species. Int J Nanomedicine 2015;11:55–68.
61. Ghasemi P, Shafiee G, Ziamajidi N, Abbasalipourkabir R. Copper

nanoparticles induce apoptosis and oxidative stress in SW480 human colon cancer cell line. Biol Trace Elem Res 2023;201:3746–54.
62. Chandrakala V, Aruna V, Angajala G. Review on metal nanoparticles as nanocarriers: Current challenges and perspectives in drug delivery systems. Emergent Mater 2022;5:1593–615.
63. Vassal M, Rebelo S, Pereira M de L. Metal oxide nanoparticles: Evidence of adverse effects on the male reproductive system. Int J Mol Sci 2021;22:8061.
64. Mahdavinezhad F, Gharaei R, Farmani AR, Hashemi F, Kouhestani M, Amidi F. The potential relationship between different human female reproductive disorders and sperm quality in female genital tract. Reprod Sci 2022;29:695-710.
65. Klein JP, Mery L, Boudard D, Ravel C, Cottier M, Bitounis D. Impact of nanoparticles on male fertility: what do we really know? A systematic review. Int J Mol Sci 2022;24:576.
66. Farmani AR, Mahdavinezhad F, Scagnolari C, Kouhestani M, Mohammadi S, Ai J, *et al*. An overview on tumor treating fields (TTFields) technology as a new potential subsidiary biophysical treatment for COVID-19. Drug Deliv Transl Res 2022;12:1605-15.
67. Nica V, Marino A, Pucci C, Şen O, Emanet M, De Pasquale D, *et al*. Cell-membrane-coated and cell-penetrating peptide-conjugated trimagnetic nanoparticles for targeted magnetic hyperthermia of prostate cancer cells. ACS Appl Mater Interfaces 2023;15:30008–28.
68. Sharma SK, Bagshawe KD. Translating antibody directed enzyme prodrug therapy (ADEPT) and prospects for combination. Expert Opin Biol Ther 2017;17:1–13.